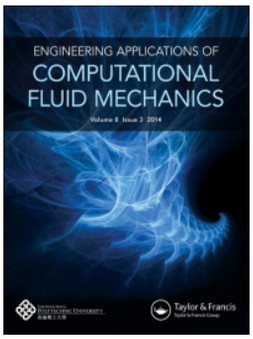

Taylor & Francis
Taylor & Francis Group

Engineering Applications of Computational Fluid Mechanics

ISSN: (Print) (Online) Journal homepage: www.tandfonline.com/journals/tcfm20

Modelling flame-to-fuel heat transfer by deep learning and fire images

Caiyi Xiong, Zilong Wang & Xinyan Huang

To cite this article: Caiyi Xiong, Zilong Wang & Xinyan Huang (2024) Modelling flame-to-fuel heat transfer by deep learning and fire images, Engineering Applications of Computational Fluid Mechanics, 18:1, 2331114, DOI: 10.1080/19942060.2024.2331114

To link to this article: https://doi.org/10.1080/19942060.2024.2331114

Published online: 21 Mar 2024.

ENGINEERING APPLICATIONS OF COMPUTATIONAL FLUID MECHANICS
2024, VOL. 18, NO. 1, 2331114
https://doi.org/10.1080/19942060.2024.2331114

Taylor & Francis
Taylor & Francis Group

Modelling flame-to-fuel heat transfer by deep learning and fire images

Caiyi Xiong[a], Zilong Wang[b] and Xinyan Huang[b]

[a]School of Mechanical and Automotive Engineering, South China University of Technology, Guangzhou, People's Republic of China; [b]Research Centre for Fire Safety Engineering, Department of Building Environment and Energy Engineering, The Hong Kong Polytechnic University, Kowloon, Hong Kong

ABSTRACT

In numerical fire simulations, the calculation of thermal feedback from the flame to the solid and liquid fuel surface plays a critical role as it connects the fundamental gas-phase flame burning and condensed-phase fuel gasification. However, it is a computationally intensive task in CFD fire modelling methods because of the requirement of a high-resolution grid for calculating the interface heat transfer. This paper proposed a real-time prediction of the flame-to-fuel heat transfer by using simulated flame images and a computer-vision deep learning method. Different methanol pool fires were selected to produce the image database for training the model. As the pool diameters increase from 20 to 40 cm, the dominant flame-to-fuel heat transfer shifts from convection to radiation. Results show that the proposed AI algorithm trained by flame images can predict both the convective and radiative heat flux distributions on the condensed fuel surface with a relative error below 20%, based on the input of real-time flame morphology that can be captured by a larger grid size. Regardless of growing or decaying fires or puffing flames induced by buoyancy, this method can further predict the non-uniform distribution of heat transfer coefficient on the interface rather than using empirical correlations. This work demonstrates the use of AI and computer vision in accelerating numerical fire simulation, which helps simulate complex fire behaviours with simpler models and smaller computational costs.

Highlights

- A total framework between AI model and fire simulation software is designed to further enhance the reliability of AI-based fire simulations.
- A standard pool fire simulation database is built using numerical model recommend by the IAFSS Computation Group.
- A deep learning model is developed to predict both the convective and radiative heat flux distributions on the condensed fuel surface using numerical images database.
- The demonstration showcases the application of AI and computer vision to accelerate numerical fire simulation.

ARTICLE HISTORY
Received 4 January 2024
Accepted 11 March 2024

KEYWORDS
Fire simulation; artificial intelligence; fire image process; heat transfer; pool fire; computer vision

1. Introduction

Fire engineers and researchers nowadays rely strongly on the use of Computational Fluid Dynamics (CFD) methods to reveal intricate combustion dynamics and explain complex flame behaviours, e.g. ignition, fire spread (Cui et al., 2023), and extinction (Cox, 1994). As a result, the CFD-based fire modelling has been playing important roles not only in scientific research, but also in engineering applications such as fire risk analysis, fire safety design and firefighting operations (Vidmar & Petelin, 2007).

In fire simulation, accurate prediction of boundary layer combustion (Khalil et al., 2019; Tieszen, 2001) is important because it captures the interaction between gas-phase flame and condensed-phase fuels and supports the fire triangle (Drysdale, 1998). Within this context, an accurate calculation of the flame-to-fuel heat transfer (primarily includes convection and radiation) on the boundary layer and interface (Xie et al., 2021) is essential for modelling the combustion process and reproducing fire phenomena.

In experimental investigations pertaining to heat transfer, the utilisation of heat flux gauges proves to be a convenient method for measurement. Silvani and Morandini (2009) employed a thermocouple in

CONTACT Zilong Wang zilong.wang@connect.polyu.hk; Xinyan Huang xy.huang@polyu.edu.hk

conjunction with two heat flux gauges, specifically radiant and total gauges, to effectively measure temperature and heat fluxes during the propagation of fire across diverse vegetative fuels. Hao et al. (2020) conducted a comprehensive study on the combustion of wood under varying heat flux conditions using a cone calorimeter. Zhang et al. (2021) focused on examining the impact of flame attachment behaviours on heat flux, employing a heat flux metre for the purpose of analysis. Ji et al. (2021) delved into investigating the flame radiation characteristics of pool fires and subsequently developed a novel model based on the classical solid flame model to predict radiative heat flux. These studies collectively contribute to the advancement of knowledge in the field of heat transfer analysis in fire scenarios.

However, such heat-transfer process is rarely resolved in large-scale fire simulation, because solving thin boundary layer requires a fine grid size (0.1–1 mm) and massive computational time. Thus, conventional heat transfer correlations, such as the Nusselt number-based convection coefficient (Quintiere, 2006), are used to yield a constant heat flux. However, most of the empirical correlations for heat transfer are not established from real fire test, and turbulent fire is not steady but oscillates by buoyancy. Thus, there is a need for a rapid and real-time determination of the flame-to-fuel heat transfer.

To resolve the complex flame-to-fuel heat transfer, different modelling techniques and assumptions have been applied. For example, a convective model normalised by pyrolysis mass flux, proposed by Li and Hostikka (2019), shows the necessity in Large Eddy Simulation (LES) for reproducing the upward flame spread over birch rods. Ahmed and Trouvé (2021) also demonstrated that a radiative flux incorporating a prescribed radiant fraction is essential for capturing the heat feedback on pool fire surfaces. Huang et al. (2017) input the transient heat flux measured from experiments to predict the burning rate of wood with only a solid-phase model. Nevertheless, new methods that can be easily adopted in CFD codes and generalised for more fire processes are still needed.

Fire images, captured by camera and cellphone, offer an indirect way to assess the relevant fire parameters (Hu et al., 2017; Xiong et al., 2022). These images contain information like fire structure, length scale, colour, puffing, and fuel shape. Previous studies have successfully used fire images to determine critical parameters involved in burning, like fire spread rate (Huang & Gao, 2021), heat release rate (HRR) (Roper, 1977), fuel regression rate (Xiong et al., 2022), and fuel mass flux (Xiong et al., 2022). Fundamentally, fire size and shape are mainly controlled by the fire HRR or gaseous fuel, while insensitive to the heat transfer on the flame-to-fuel interface. That is, CFD simulations with large cells can still accurately capture the fire image, size, and shape (see Figure 1).

Then, it is worth exploring the real-time prediction of flame-to-fuel heat transfer using some coefficients associated with fire size and shape. If successful, the predicted values can be used in CFD simulations with coarse grids, which can reduce the computational cost without losing accuracy. However, traditional image-processing methods usually rely strongly on image resolution, and their processing based on pixel analysis is often time-consuming (Xiong et al., 2022), posting challenges for real-time image processing.

Under the rapid development of artificial intelligence (AI) technology, deep learning algorithms and computer vision (CV) methods have been widely used in fire research. Hodges et al. (2019) utilised transpose convolutional neural networks (TCNN) to predict spatially resolved temperatures and velocities in compartment fires. Similarly, (Wu, et al., 2020; Wu, et al., 2022; Wu, et al., 2022) employed deep learning to forecast tunnel fire development and smoke transportation 60 s in advance, showcasing its application in a laboratory-scale tunnel model for smart firefighting systems. Additionally, (Zhang, et al., 2022; Zhang, et al., 2022) employed AI for training temperature sensor data to forecast the occurrence of flashover. In terms of computer vision, it has been effectively employed in fire detection (Wang, et al., 2023) and segmentation (Wang, et al., 2023). (Wang, et al., 2022; Wang, et al., 2022) also harnessed AI for training in smoke and fire image identification, enabling real-time fire information assistance in firefighting scenarios. AI methods have helped reveal hidden information in complex physical processes, including fluid and combustion dynamics (Vinuesa & Brunton, 2022; Wan et al., 2021; Wang, et al., 2023; Yellapantula et al., 2021). Nevertheless, few attempts have been made to predict the flame-to-fuel heat transfer by AI agent that is trained by fire images. The AI prediction can largely reduce the reliance of fire simulation on fine grid size and enable the use of course mesh to accurately reveal complex fire phenomena, see Figure 2.

This paper aims to use numerical fire images and AI method to predict real-time heat transfer between flame and condensed fuel. The heat transfer coefficients on the flame-to-fuel interface will be predicted by AI and CV and then compared with empirical coefficients. This work has the potential to advance the AI-assisted fire simulation technique and reduce the computational cost without sacrificing accuracy.

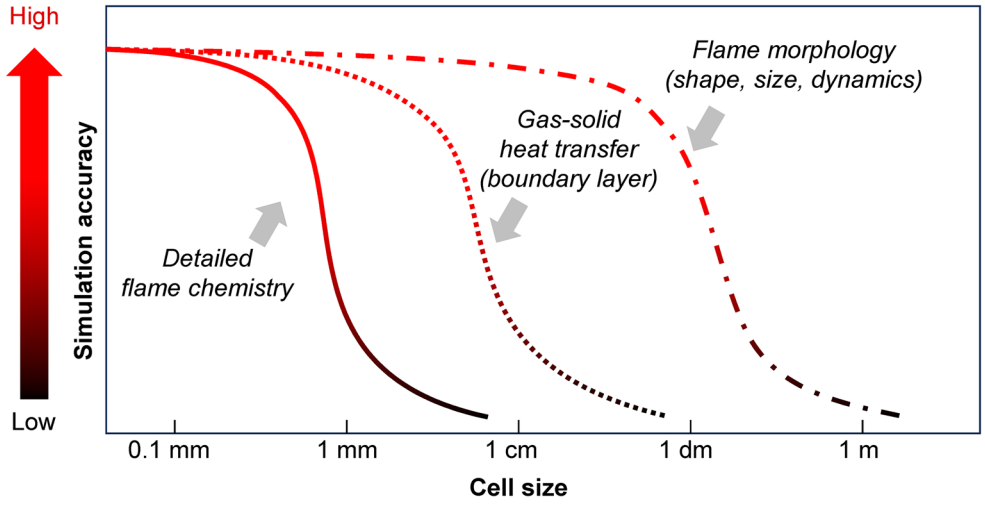

Figure 1. Sensitivity of modelling accuracy of different fire processes to cell size.

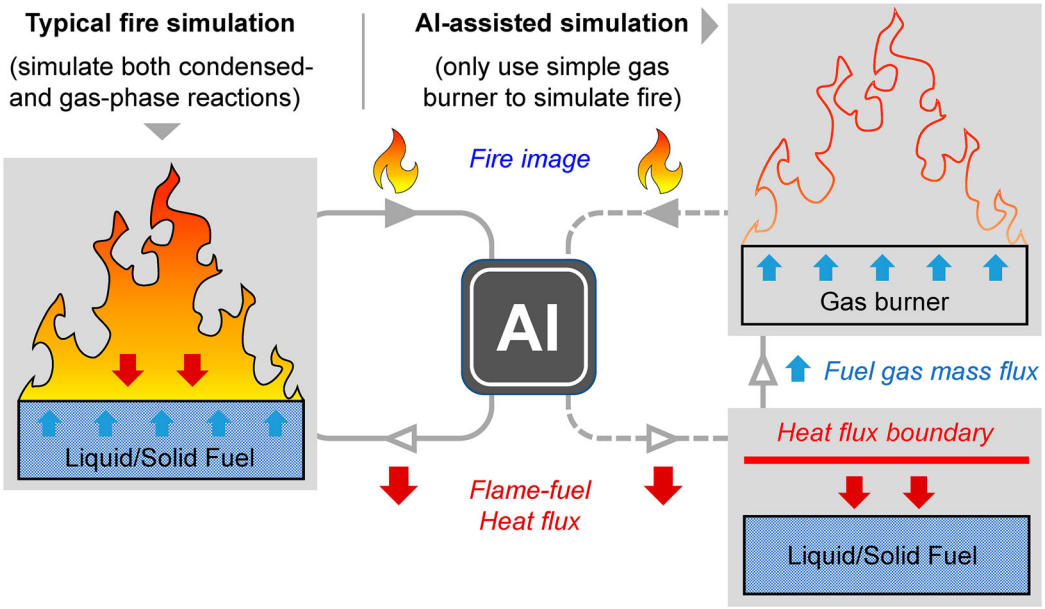

Figure 2. Basic idea of AI-accelerated fire simulation.

2. Methodology

The fundamental premise of this study involves the construction of an extensive fire simulation database. Then, the data serve as input for AI training to establish the intricate relationship between fire image and flame-to-fuel heat transfer. Ultimately, the trained AI model predicts the heat flux distribution on the condensed fuel surface in analogous burning scenarios, also seen in Figure 2.

2.1. Numerical model set-up

The current simulation employed Fire Dynamics Simulator (FDS 6.7.8) (McGrattan et al., 2020), an LES solver developed by NIST, which has been extensively used to simulate the fire-burning process. The current simulation targets a medium-scale pool fire featuring a 30-mm circular pan filled with methanol. This configuration can produce a moderate Reynolds number flow field and a less sooty fire. It is also adopted by the 'IAFSS Working Group on Measurement and Computation of Fire Phenomenon' as one of the targets used for validating fire simulation (Brown et al., 2018). To enrich the fire image database, additional simulations with pool diameters ranging from 20 to 40 cm will also be carried out.

The numerical set-up follows the methanol pool fire simulation in the FDS Validation Guide (McGrattan et al., 2013). As seen in Figure 3(a), a 3-D domain with a size of 0.6 m (length) × 0.6 m (width) × 1.2 m (height) was used. The fuel pool was placed on the ground and aligned with the bottom centre. All domain boundaries

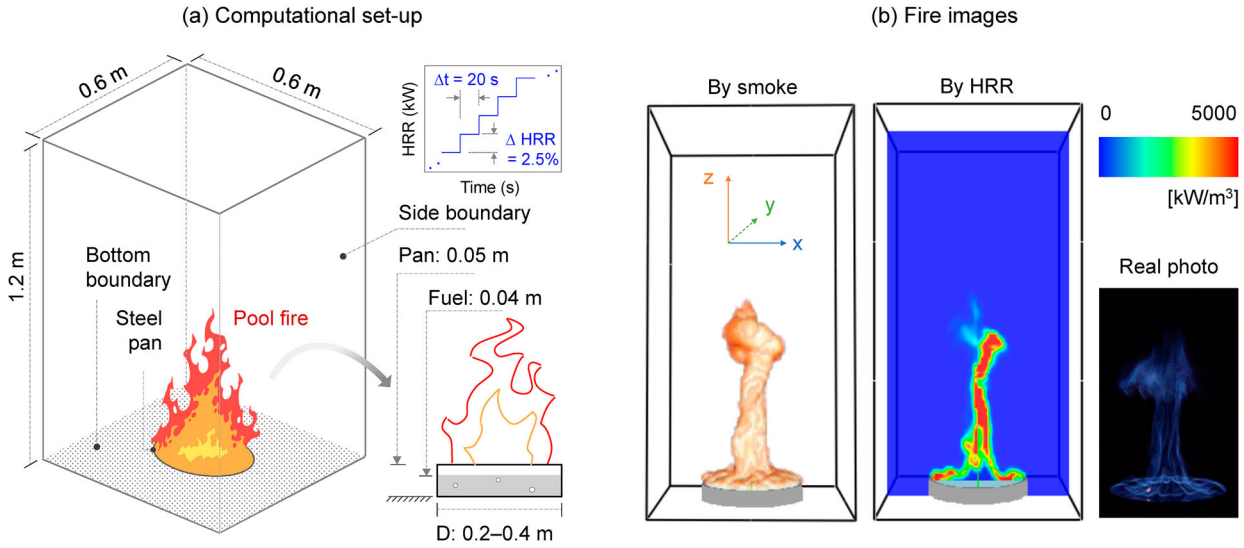

Figure 3. (a) Schematic of the computational set-up, and (b) fire images on a 30-cm methanol pool by spurious smoke (left), HRR contours (middle), and experimental photo (right).

were left open to replicate the experiment (Chan et al., 2019) in which the fuel pool is elevated above the floor, allowing airflow to supply from all directions.

As recommended by (Chan et al., 2019), the circular pool was set to be made of 1-mm thick steel plates. The pool rim has a height of 0.05 m, into which 0.04-m thick of liquid methanol is filled. The chemical reaction between methanol and air was simulated using a two-step chemistry, where both reactions were sequentially performed assuming fast kinetics. It was also assumed that no soot formation occurred during either reaction. The physical properties of methanol were obtained from the data sheet published by the Methanol Institute (Methanex.com, 2012). Furthermore, the CFD model employed in this study predicted the radiative fraction for all cases, eliminating the need for user specification. The fuel release mass flux, $\dot{m}''$, is key to quantify pool burning. Here, $\dot{m}''$ was set as a function of the pool diameter, D, following the expression (Chen et al., 2023):

$$\dot{m}'' = \dot{m}''_{\infty}(1 - e^{-k\beta D}) \tag{1}$$

where $(1 - e^{-\kappa\beta D})$ is the effective volume emissivity, and $\dot{m}''_{\infty}$ is the maximum asymptotic burning flux of a hypothetical infinite pool fire. In this work, $\dot{m}''_{\infty} = 21\ \mathrm{g/m^2\text{-}s}$ and $\kappa\beta = 2.98\ \mathrm{m^{-1}}$, as recommended by (Quintiere, 2006).

The convergence study suggested a uniform grid with a spatial step of 0.01 m or smaller to resolve the pool fire. To ensure simulation accuracy and collect enough data for AI training, a uniform mesh with a spatial resolution of 0.01 m was adopted. Each model calculates for 800 s, during which the fuel mass flux $\dot{m}''$ ranges from zero to the maximum with an increase of 2.5% at every 20 s, so to cover the fire images at different developing stages, also see Figure 3(a).

2.2. Simulated fire images and behaviours

The FDS program offers various ways to generate fire images. The most common one is from the iso-surfaces of 'smoke-temperature', see Figure 3(b), but it might be distorted due to the use of an assumed mass extinction coefficient of sooty solid materials to compute spurious smoke generation (McGrattan et al., 2020), thereby not applicable to a less sooty methanol fire. Instead, we used the counters of fire HRR to depict the fire structure. Note that in 3-D simulation, one can observe the projected plane of fire from any angle of view. To observe more details, the HRR counters on the vertical plane across the pool centre were used as the fire image, which shows similarity to the real fire photos, as compared in Figure 3(b). Here, the projection on the x-z plane was used to represent the fire size and shape, given that pool fires often behave in an axisymmetric manner.

To further confirm if these numerical fire images outlined by HRR contour can accurately reflect pool fire behaviours, two parameters including the fire puffing frequency and averaged height were examined for 20–40 cm pools and compared with experiments (Drysdale, 1998). Figure 4 shows both parameters follow the experimental fittings (Drysdale, 1998), proving the reliability of the simulations.

2.3. Dataset pre-processing

It is also necessary to check whether the pool model can simulate accurate heat transfer between flame and fuel

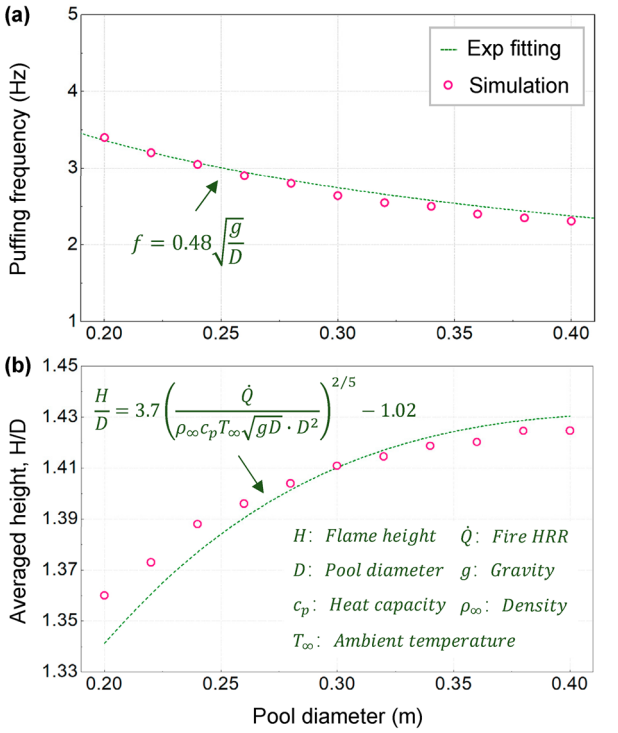

Figure 4. Comparisons of simulated (a) fire puffing frequency and (b) averaged height with experiment (Drysdale, 1998).

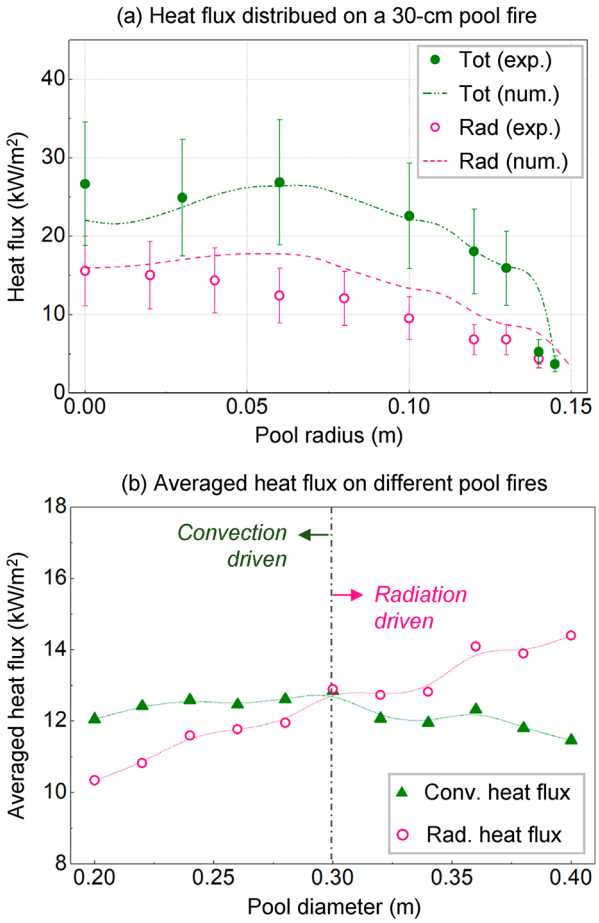

Figure 5. (a) Comparison of simulation and experiments (Chan et al., 2019; Klassen et al., 1994) for the total and radiative heat flux distributed on a 30-cm pool fire surface, and (b) comparison of averaged convective and radiative heat flux on the surfaces of all pool simulations.

during burning. Figure 5 took a 30-cm pool as an example and compared the simulated radiative ($\dot{q}''_{rad}$) and total heat flux ($\dot{q}''_{tot}$) time-averaged over three puffing cycles with validation experiments (Chan et al., 2019; Klassen et al., 1994).

Note that FDS does not directly export the value of convective heat flux, but it can be calculated by the difference between total and radiative flux. Still, a reasonable agreement between simulations and experiments can be seen in Figure 5(a), suggesting that the pool fire model can yield reliable flame-fuel heat transfer data. The small deviation can be attributed to the fact that the experiments are measured not on the fuel surface but 7-mm above it.

To confirm that simulations of other 20–40 cm pool fires can also yield reliable heat flux data, Figure 5(b) examined the averaged radiative and convective heat flux over the fuel surface in all pool-fire cases. As seen, the dominant heat transfer will change from convection to radiation when the pool diameter exceeds 30 cm. This trend agrees well with the previous experimental measurements (Maragkos & Beji, 2021), in which the critical pool size to affect the dominant mode of heat transfer was found to be also around 30 cm.

2.4. Fire image pre-processing

Due to the buoyancy-induced puffing, both the fire shape and its heat flux to condensed fuel will constantly change over time, even when the fuel burning rate ($\dot{m}''$) is near constant. To comprehensively capture diverse flame characteristics, 200 image frames are randomly selected at every 20 s during simulation while step-likely increasing $\dot{m}''$. Such a process can encompass a broad spectrum of flame image features associated with identical pool size and heat flux data. Consequently, a database is meticulously curated, comprising a total of 90,200 flame images. Each set of 200 flame images within the database corresponds on a one-to-one basis with the transient radial heat flux distribution, thereby elucidating the burning characteristics inherent to each pool size and $\dot{m}''$.

Based on this fire-image database, a requisite data preprocessing protocol is implemented to optimise the data for training AI model to discern fire-related information, see Figure 6(a). First, it is imperative to extract image

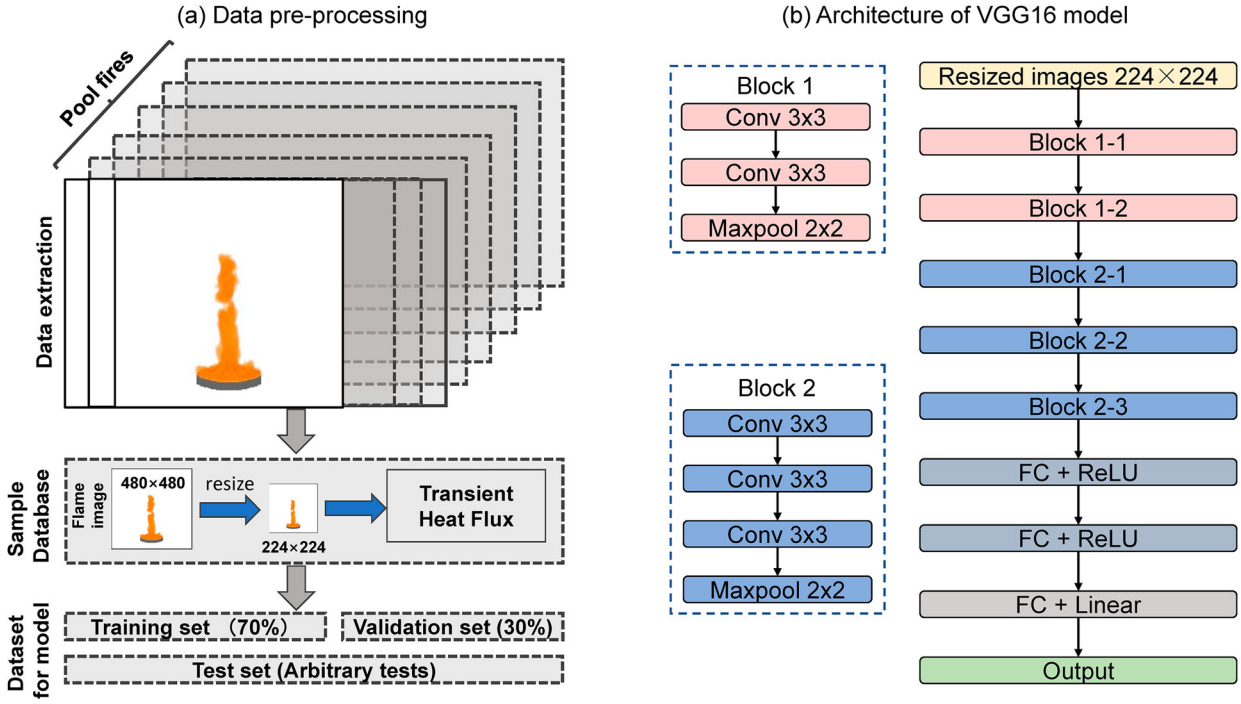

Figure 6. (a) Pre-processing for data training, validation, and test; and (b) architecture of VGG-16 for real-time heat transfer prediction based on fire images.

clips and retain solely the fire parts. The most extensive fire area within the database serves as a reference to standardise the scale across all images. As a result, a fire area with 480 × 480 pixels is delineated as the target region for training the AI model.

Then, the amalgamation of these images and the corresponding heat flux distribution will constitute the AI training dataset, which is further bifurcated into two distinct subsets: (1) the training set, encompassing 70% of the data and is utilised for the actual training of the model; and (2) the validation set, comprising the remaining 30% data, which serves to evaluate the model performance during the training process. Notably, the training process involves the development of two distinct AI models, one for predicting the total heat flux and another for radiation, resulting in two distinct model outputs.

2.5. Deep learning algorithm

While flame images can depict variations in heat flux distribution, human visual perception struggles to discern nuanced flame characteristics. Among various CNN models, this work employed VGG-16 (Simonyan & Zisserman, 2015) architecture to extract fire characteristics under various pool scenarios and build their relation with flame-fuel heat flux. Unlike conventional image processing algorithms necessitating manual feature extraction, CNN inherently captures spatial and temporal dependencies following adequate training. This algorithm was initially developed by the Visual Geometry Group at Oxford, standing out for its deep architecture and superior performance in computer vision tasks (Ahmadvand et al., 2017; Chen et al., 2019). The VGG-16 architecture, denoted by its name, signifies the presence of 16 layers, encompassing 13 convolutional layers and 3 fully connected layers. VGG-16 has gained recognition as a benchmark in CV and deep learning due to its straightforward design comprising small convolutional filters. Originally developed for image classification tasks, this study deviates from convention by modifying the activation function of the final layer. Specifically, the Softmax activation function is replaced with the Rectified Linear Unit (ReLU) activation function to facilitate the output of heat flux values.

The detailed configuration of VGG-16 used is depicted in Figure 6(b). The processed flame images, with dimensions of 224 × 224 × 3, serve as input to VGG-16 architecture, generating feature maps representative of the fire structures. These feature maps then undergo flattening into a column vector to establish a non-linear relationship with the heat flux output through fully connected layers. The comprehensive network structure encompasses 41 million parameters, facilitating the nuanced extraction of features from each image. Rectified Linear Unit (ReLU) is employed as the activation function in both convolutional and fully connected layers, with the final layer utilising Linear activation. Mean Squared Error (MSE), Mean Absolute Percentage Error (MAPE)

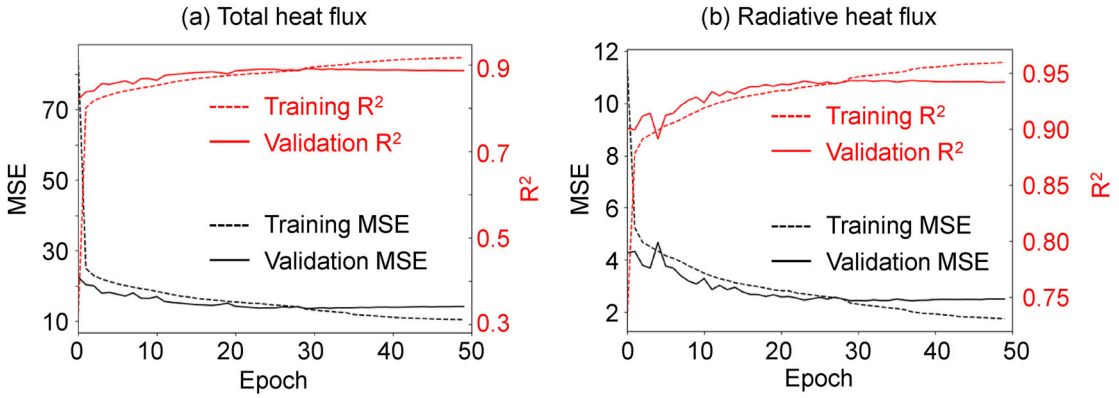

Figure 7. MSE and R^2 losses of training and validation during the training process for the AI model of (a) total heat flux and (b) radiative heat flux.

and R^2 (Equations 2–5) serve as loss functions to gauge disparities between actual (FDS simulation) and predicted values, where y_i is the predicted heat flux, and $\widehat{y_i}$ is the simulated heat flux. Dropout, with a rate of 0.2, is applied after each max pooling and fully connected layer to mitigate overfitting. Model computations are executed on a server equipped with 32 CPU cores and a Tesla P100 GPU card, requiring approximately one day for 50-step training.

$$MAE = \frac{1}{n}\sum_{i=1}^{n}|y_i - \widehat{y_i}| \tag{2}$$

$$MSE = \frac{1}{n}\sum_{i=1}^{n}(y_i - \widehat{y_i})^2 \tag{3}$$

$$MAPE = \frac{1}{n}\sum_{i=1}^{n}\left|\frac{y_i - \widehat{y_i}}{y_i}\right| \times 100\% \tag{4}$$

$$R^2 = 1 - \frac{\sum_{i=1}^{n}(y_i - \widehat{y_i})^2}{\sum_{i=1}^{n}(y_i - \bar{y})^2} \tag{5}$$

3. Results and discussion

3.1. Model training

The performance trajectories of the models during the training phase are presented in Figure 7. As can be seen, the deep learning models can achieve convergence following 50 training iterations, manifesting the minimal MSE loss of 13.6 and maximum R^2 of 0.89 for predicting total heat flux, with MSE of 2.4 and R^2 of 0.94 for radiation. These outcomes signify the adept capability of the deep learning models in accurately predicting transient heat flux distributions on the fuel surface within the confines of the training dataset.

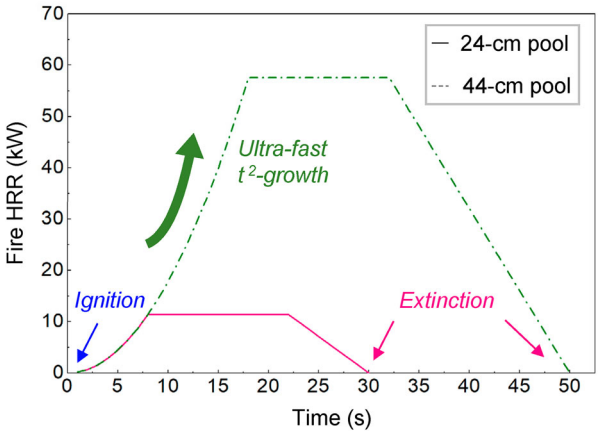

Figure 8. HRR curves of two additional pool fire simulations from ignition to extinction.

3.2. Predicting transient heat flux

After training, the AI agent can be further used in more complex simulations. Two more pool cases that cover the whole burning stages from ignition to extinction were then carried out. Figure 8 shows their HRRs developing first following the ultra-fast t^2-fire growth model (Drysdale, 1998), and then keeping stable for another duration, and finally dropping to extinction. Note that these two pool diameters were 24 cm (convection control) and 44 cm (radiation control). The former is interpolation, while the latter is extrapolation.

Figure 9 first plots the spatiotemporal evolutions of the total and radiative heat flux distributions predicted by the deep-learning model. Details of this prediction can be seen in Video S1 (https://doi.org/10.6084/m9.figshare.24941544.v1). In Figure 9, the simulation time is advanced along the upward direction of the vertical axis. Thus, a horizontal line at any location represents the instantaneous radical heat flux distribution at this moment. Likewise, a vertical line along an arbitrary location shows

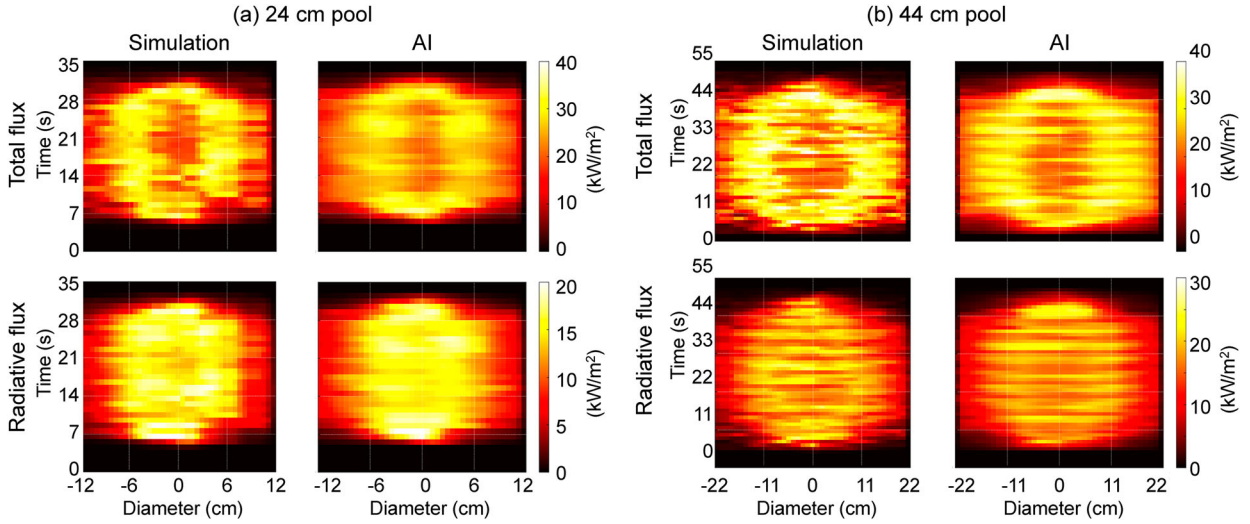

Figure 9. Heat maps of total and radiative heat flux predicted for (a) 24-cm and (b) 44-cm pool fires. See Video S1.

the temporal variation in the heat flux at a specific fuel location.

The most prominent feature in Figure 9 is that regardless of the form in which the fire HRR evolves, the AI model can well predict the variation in flame-fuel heat flux in real-time. Such a feature exhibits suitability not only for the 24-cm pool within the training size, demonstrating a relative error of less than 10%, but also for the larger 44-cm pool fire, exhibiting a relative error of less than 20%. This indicates that the mapping relationship established between fire images and heat flux has the potential to be extrapolated for use even in fires outside the training size.

Another feature in the heat maps in Figure 9 is that the prediction of heat flux distribution still fluctuates after both fire HRRs have entered a stable and fully developed stage. This demonstrates that the AI model can capture the heat flux variation not only caused by fire growth or decay but also by fire puffing. To verify this, Figure 10 further plots the total and radiative heat flux at the pool centre versus time, combined with the original FDS simulation data presented for comparison. A comprehensive comparison is presented in Table 1, highlighting the agreement between the simulation and prediction results. Notably, a high degree of concordance between the simulated values and predictions is evident in the case of the 24 cm pool fire, with MAE of 1.6 and 2.8 kW/m^2. Despite exceeding the maximum size of the database pool fire, the AI model also exhibits commendable predictive performance for the 44-cm pool fire, yielding MAE values of 3.3 and 4.9 kW/m^2. Importantly, all predictive results demonstrate a relative error below 20%. Meanwhile, the larger the fire size, the greater the heat flux predicted. This observation also follows the trend observed in previous tests or simulations, further demonstrating the strong dependence of the heat flux predictions on fire images in the current AI model.

Table 1. Comparison between FDS simulation and AI prediction at the pool centre.

	Radiative heat flux		Total heat flux	
Diameter (cm)	24	44	22	44
MSE	5.3	18.0	16.5	45.2
MAE (kW/m^2)	1.6	3.3	2.8	4.9
MAPE (%)	0.4	0.6	7.1	20.5
R^2	0.88	0.72	0.85	0.66

3.3. AI prediction of convective coefficient

In most fire simulations and experiments, the total heat transfer coefficient (h) and its convective component (h_c) are always treated uniformly and empirically and given as constant. As the current AI method can capture heat flux based on fire images, it should be also able to predict the transient distribution of the convective coefficients over fuel surface.

The extra 24-cm and 44-cm pool fires are again taken as examples. The detailed predictions of h and h_c distributed over the fuel surface versus time were plotted in Figure 11. Here, the local h and h_c are given by:

$$h = \dot{q}''_{tot}/(T_g - T_w) \tag{6}$$

$$h_c = (\dot{q}''_{tot} - \dot{q}''_{rad})/(T_g - T_w) \tag{7}$$

where T_g is the gas temperature on the interface, and $T_w = 338$ K is the methanol boiling point. For comparison, the empirical free convection coefficient was calculated by Nu number ($Nu = 0.11Re^{1/2}Pr^{2/3}$) (Drysdale, 1998) using the pool diameter and buoyancy

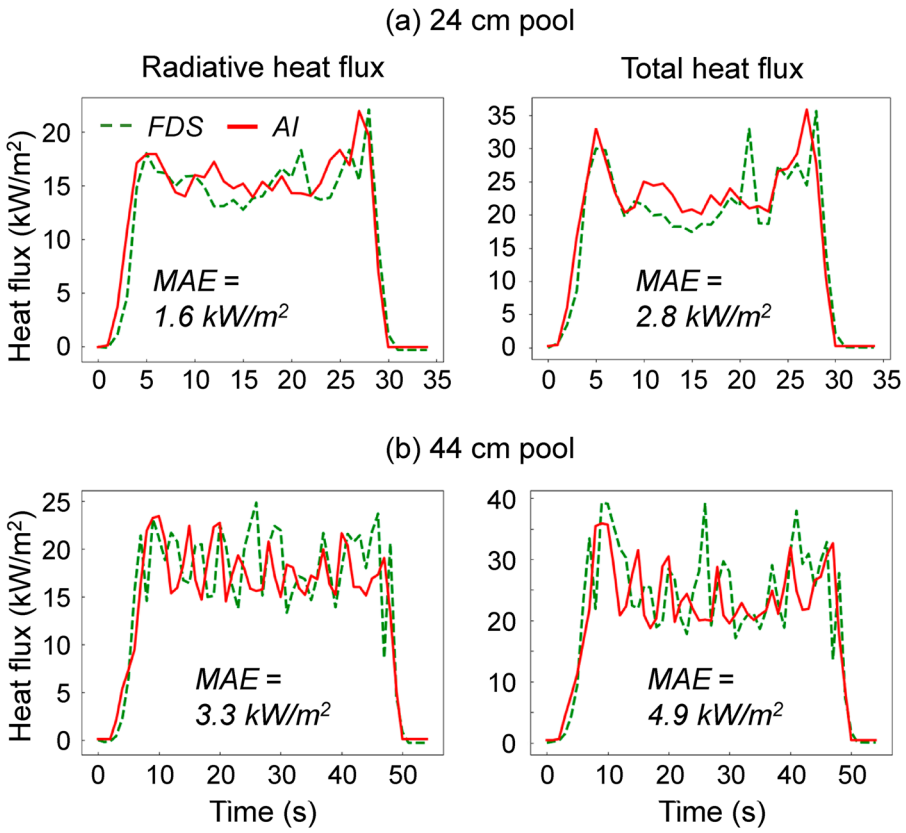

Figure 10. Comparison of radiative and total heat flux history from FDS simulation and AI prediction at the centres of (a) 24-cm and (b) 44-cm pool fires.

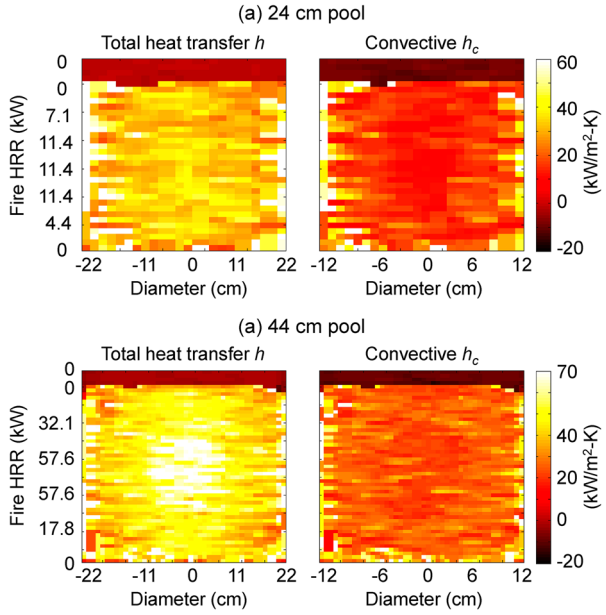

Figure 11. Heat maps of total and convective heat transfer coefficients predicted for (a) 24-cm and (b) 44-cm pool fires versus the time histories of fire HRR.

velocity as characteristic parameters. That is, h_c^* (24-cm) = 21.7 kW/m^2-k and h_c^* (44-cm) = 34.6 kW/m^2-k, respectively.

It can be seen from Figure 11 that the predicted h_c has a similar value to h_c^* in both cases, especially at the stable burning stage but exhibits a non-uniform distribution rather than being constant. As expected, the total coefficient h has a higher value than its convective component h_c, and both the highest h and h_c occur near the pool edge where air is entrained. Also, after extinction, the values of both h and h_c become negative because they change to environmental cooling. Thus, if the constant h_c^* can be replaced by a transient h or h_c curve, the simulation accuracy may be further improved, which needs future investigations.

3.4. Perspective of AI-accelerated fire simulation

On the ground of the above discussions, it allows to conclude that the proposed AI-driven method could assist future CFD fire modelling in several aspects:

(1) **Cell size:** by predicting heat flux on the flame-to-fuel interface, a large cell size or fewer number of total cells can be adopted in fire modelling without resolving the boundary layer on the condensed fuel (see Figure 1); and

(2) **Need of CFD:** Given a flame image, both the convective and radiative heat transfer coefficients on the interface of any fuel can be directly predicted without the need for CFD calculation; and
(3) **Solid phase modelling:** One can directly evaluate the fuel burning mass flux using the predicted interface heat flux (see Figure 2), based on which it is possible to simulate complex flame behaviours, such as flame heating, piloted ignition, and flame spread, without using the detailed condensed-phase model of pyrolysis or evaporation (Hodges et al., 2023).

The above advantages possess significant potential applications in future fire simulation research and engineering design practices. For example, in large-scale fire simulations, coarse grids can be employed with the AI method to calculate an accurate flame shape and fire power, allowing one to obtain more precise temperature fields or thermal radiation for evaluating the yield ignition risk or thermal damage in the environment. Moreover, for modelling piloted ignition and fire spread, AI model trained by flame image can also predict the thermal feedback that fuel receives and, consequently, achieve direct prediction of the ignition time by flame and fire spread rate.

Nevertheless, the current work solely proposes the idea and some simple examples to demonstrate the AI-accelerated fire simulation. Several limitations remain to be addressed in this study. Firstly, while the proposed method demonstrates applicability in simulations employing a moderately coarse grid, excessively coarse grids may lead to alterations in the flame shape. Therefore, careful consideration should be given to grid resolution to avoid compromising the accuracy of the simulation results. Secondly, it is important to note that the effectiveness of the heat flux prediction heavily relies on the availability of relevant data within the simulation case database. In instances where the target simulation case falls outside the scope of the database, significant errors in heat flux prediction may occur due to the lack of specific rules or established relationships within the model. Lastly, given that methanol pool fire images are utilised as the basis for analysis in this study, the effect of fuel type is not fully considered. Future investigations should be conducted to validate the effect of fuel type on heat flux prediction. There are also many technical and practical issues waiting to be addressed. For example, a tool is needed to automatically substitute the AI-predicted heat flux back into the simulation by updating the boundary condition. Can the proposed AI method be extended for predicting the heat flux in other fire processes? Further exploration of AI-driven fire modelling by more researchers is desired.

4. Conclusions

In this paper, an AI-based approach for indirect acquisition of flame-fuel thermal feedback in fire simulation was first proposed, wherein simulated fire images (HRR contours) produced by CFD code are trained in a deep learning algorithm to estimate both the convective and radiative heat fluxes on fuel surface during fire burning. The simulation targets selected methanol pool fires. By varying diameters from 20 to 44 cm, the dominant heat transfer on the fuel pool will change from convection to radiation.

Then, the flame image-based AI prediction is demonstrated to identify changes in heat flux distribution resulting from fire growth, decay, and buoyancy-induced puffing in real time. Two distinct pool fire scenarios were selected to test the AI model, encompassing one case within the range of the existing database and another case that fell outside this range. Notably, the prediction errors observed for scenarios within the database range were consistently below 10%, while the prediction errors for the out-of-range scenario remained below 20%. These findings collectively demonstrate the commendable predictive performance of the AI model for fire scenarios within the confines of the database as well as those in close proximity. This method also predicts the real-time distribution of the heat transfer coefficients on the fuel surface, giving more accurate calculations than empirical heat transfer correlations used in conventional practices. This work demonstrates the use of AI and CV in accelerating numerical fire simulation, which helps simulate complex fire behaviours with simpler models and smaller computation resources.

Acknowledgments

C.X. is funded by the National Natural Science Foundation of China (NSFC) grant number 52006185; Z.W. is funded by the SFPE Foundation Student Research Grant; X.H. is funded by the Hong Kong Research Grants Council Theme-based Research Scheme (T22-505/19-N).

CRediT authorship contribution statement

Caiyi Xiong: Methodology, Writing – Original Draft, Formal analysis. **Zilong Wang:** Methodology, Investigation, Writing – review & editing. **Xinyan Huang:** Conceptualisation, Writing – Review & Editing, Supervision.

Data availability statements

The datasets generated during and/or analysed during the current study are available from the corresponding author on reasonable request.

Disclosure statement

No potential conflict of interest was reported by the author(s).

Funding

This work was supported by National Natural Science Foundation of China [grant number 52006185]; Research Grants Council, University Grants Committee [grant number T22-505/19-N]; SFPE Foundation [grant number Student Research Grant].

References

Ahmadvand, P., Ebrahimpour, R., & Ahmadvand, P. (2017). How popular CNNs perform in real applications of face recognition. *2016 24th Telecommunications Forum (TELFOR)*. https://doi.org/10.1109/TELFOR.2016.7818876

Ahmed, M. M., & Trouvé, A. (2021). Large eddy simulation of the unstable flame structure and gas-to-liquid thermal feedback in a medium-scale methanol pool fire. *Combustion and Flame*, *225*, 237–254. https://doi.org/10.1016/j.combustflame.2020.10.055

Brown, A., Bruns, M., Gollner, M., Hewson, J., Maragkos, G., Marshall, A., McDermott, R., Merci, B., Rogaume, T., Stoliarov, S., Torero, J., Trouvé, A., Wang, Y., & Weckman, E. (2018). Proceedings of the first workshop organized by the IAFSS Working Group on Measurement and Computation of Fire Phenomena (MaCFP). *Fire Safety Journal*, *101*, 1–17. https://doi.org/10.1016/j.firesaf.2018.08.009

Chan, S. K., Lee, K. Y., & Hamins, A. (2019). Energy balance in medium-scale methanol, ethanol, and acetone pool fires. *Fire Safety Journal*, *107*, 44–53. https://doi.org/10.1016/j.firesaf.2019.01.004

Chen, Y., Fang, J., Zhang, X., Miao, Y., Lin, Y., Tu, R., & Hu, L. (2023). Pool fire dynamics: Principles, models and recent advances. *Progress in Energy and Combustion Science*, *95*, 101070. https://doi.org/10.1016/j.pecs.2022.101070

Chen, Z., Khemmar, R., Decoux, B., Atahouet, A., & Ertaud, J. Y. (2019). Real time object detection, tracking, and distance and motion estimation based on deep learning: Application to smart mobility. *2019 Eighth International Conference on Emerging Security Technologies (EST)*. https://doi.org/10.1109/EST.2019.8806222

Cox, G. (1994). The challenge of fire modelling. *Fire Safety Journal*, *23*(2), 123–132. https://doi.org/10.1016/0379-7112(94)90021-3

Cui, H., Chen, J., Dong, Z., Han, Z., & Liu, Q. (2023). Numerical study of the fire-smoke temperature law in the shaft of a high-rise building under the chimney effect in winter. *Engineering Applications of Computational Fluid Mechanics*, *17*, 2222811. https://doi.org/10.1080/19942060.2023.2222811

Drysdale, D. (1998). An introduction to fire dynamics. https://doi.org/10.1016/0379-7112(86)90046-9

Hao, H., Chow, C. L., & Lau, D. (2020). Effect of heat flux on combustion of different wood species. *Fuel*, *278*, 118325. https://doi.org/10.1016/j.fuel.2020.118325

Hodges, J. L., Lattimer, B. Y., Kapahi, A., & Floyd, J. E. (2023). An engineering model for the pyrolysis of materials. *Fire Safety Journal*, *141*, 103980. https://doi.org/10.1016/j.firesaf.2023.103980

Hodges, J. L., Lattimer, B. Y., & Luxbacher, K. D. (2019). Compartment fire predictions using transpose convolutional neural networks. *Fire Safety Journal*, *108*, 102854. https://doi.org/10.1016/j.firesaf.2019.102854

Hu, L., Kuang, C., Zhong, X., Ren, F., Zhang, X., & Ding, H. (2017). An experimental study on burning rate and flame tilt of optical-thin heptane pool fires in cross flows. *Proceedings of the Combustion Institute*, *36*(2), 3089–3096. https://doi.org/10.1016/j.proci.2016.08.021

Huang, X., & Gao, J. (2021). A review of near-limit opposed fire spread. *Fire Safety Journal*, *120*, 103141. https://doi.org/10.1016/j.firesaf.2020.103141

Huang, X., Li, K., & Zhang, H. (2017). Modelling bench-scale fire on engineered wood: Effects of transient flame and physicochemical properties. *Proceedings of the Combustion Institute*, *36*(2), 3167–3175. https://doi.org/10.1016/j.proci.2016.06.109

Ji, J., Ge, F., & Qiu, T. (2021). Experimental and theoretical research on flame emissivity and radiative heat flux from heptane pool fires. *Proceedings of the Combustion Institute*, *38*(3), 4877–4885. https://doi.org/10.1016/j.proci.2020.05.052

Khalil, H. M., Eldrainy, Y. A., Abdelghaffar, W. A., & Abdel-Rahman, A. A. (2019). Increased heat transfer to sustain flameless combustion under elevated pressure conditions – a numerical study. *Engineering Applications of Computational Fluid Mechanics*, *13*, 782–803. https://doi.org/10.1080/19942060.2019.1645737

Klassen, M. E., Gore, J. P., & Kashiwagi, T. (1994). Heat feedback to the fuel surface in pool fires. *Combustion Science and Technology*, *97*(4–6), 37–62. https://doi.org/10.1080/00102209408935367

Li, K., & Hostikka, S. (2019). Embedded flame heat flux method for simulation of quasi-steady state vertical flame spread. *Fire Safety Journal*, *104*, 117–129. https://doi.org/10.1016/j.firesaf.2019.01.011

Maragkos, G., & Beji, T. (2021). Review of convective heat transfer modelling in cfd simulations of fire-driven flows. *Applied Sciences*, *11*(11), 5240. https://doi.org/10.3390/app11115240

McGrattan, K., Hostikka, S., Floyd, J., McDermott, R., & Overholt, K. J. (2013). Fire dynamics simulator, Technical reference guide Volume 3: Validation (6th ed.). *NIST Special Publication*, *3*.

McGrattan, K., Hostikka, S., McDermott, R., Floyd, J., Weinschenk, C., & Overhold, K. (2020). *Fire dynamics simulator, User's guide* (6th ed.). NIST Special Publication.

Methanex.com. (2012). Physical properties of pure methanol. *Methanex Corporation*, *1*, 638.

Quintiere, J. G. (2006). *Fundamentals of fire phenomena*. Wiley. https://doi.org/10.1002/0470091150

Roper, F. G. (1977). The prediction of laminar jet diffusion flame sizes: Part I. Theoretical model. *Combustion and Flame*, *29*, 219–226. https://doi.org/10.1016/0010-2180(77)90112-2

Silvani, X., & Morandini, F. (2009). Fire spread experiments in the field: Temperature and heat fluxes measurements. *Fire Safety Journal*, *44*(2), 279–285. https://doi.org/10.1016/j.firesaf.2008.06.004

Simonyan, K., & Zisserman, A. (2015). Very deep convolutional networks for large-scale image recognition. *3rd International Conference on Learning Representations, May 7-9, 2015, ICLR 2015 - Conference Track Proceedings* (pp. 1–14).

Tieszen, S. R. (2001). On the fluid mechanics of fire. *Annual Review of Fluid Mechanics*, *33*(1), 67–92. https://doi.org/10.1146/annurev.fluid.33.1.67

Vidmar, P., & Petelin, S. (2007). Application of CFD method for risk assessment in road tunnels. *Engineering Applications of Computational Fluid Mechanics*, *1*, 273–287. https://doi.org/10.1080/19942060.2007.11015199

Vinuesa, R., & Brunton, S. L. (2022). Enhancing computational fluid dynamics with machine learning. *Nature Computational Science*, *2*(6), 358–366. https://doi.org/10.1038/s43588-022-00264-7

Wan, K., Barnaud, C., Vervisch, L., & Domingo, P. (2021). Machine learning for detailed chemistry reduction in DNS of a syngas turbulent oxy-flame with side-wall effects. *Proceedings of the Combustion Institute*, *38*(2), 2825–2833. https://doi.org/10.1016/j.proci.2020.06.047

Wang, Y., Dong, W., Liang, W., Yang, B., & Law, C. K. (2023). Predicting octane number from species profiles: A deep learning model. *Proceedings of the Combustion Institute*, *39*(4), 5269–5277. https://doi.org/10.1016/j.proci.2022.08.015

Wang, Z., Ding, Y., Zhang, T., & Huang, X. (2023). Automatic real-time fire distance, size and power measurement driven by stereo camera and deep learning. *Fire Safety Journal*, *140*, 103891. https://doi.org/10.1016/j.firesaf.2023.103891

Wang, Z., Zhang, T., & Huang, X. (2022). Predicting real-time fire heat release rate based on flame images and deep learning. *Proceedings of the Combustion Institute*. https://doi.org/10.1016/j.proci.2022.07.062

Wang, Z., Zhang, T., & Huang, X. (2023). Explainable deep learning for image-driven fire calorimetry. *Applied Intelligence*. https://doi.org/10.1007/s10489-023-05231-x

Wang, Z., Zhang, T., Wu, X., & Huang, X. (2022). Predicting transient building fire based on external smoke images and deep learning. *Journal of Building Engineering*, *47*, 103823. https://doi.org/10.1016/j.jobe.2021.103823

Wu, X., Park, Y., Li, A., Huang, X., Xiao, F., & Usmani, A. (2020). Smart detection of fire source in tunnel based on the numerical database and artificial intelligence. *Fire Technology*. https://doi.org/10.1007/s10694-020-00985-z

Wu, X., Zhang, X., Huang, X., Xiao, F., & Usmani, A. (2022). A real-time forecast of tunnel fire based on numerical database and artificial intelligence. *Building Simulation*, *15*(4), 511–524. https://doi.org/10.1007/s12273-021-0775-x

Wu, X., Zhang, X., Jiang, Y., Huang, X., Huang, G. G. Q., & Usmani, A. (2022). An intelligent tunnel firefighting system and small-scale demonstration. *Tunnelling and Underground Space Technology*, *120*, 104301. https://doi.org/10.1016/j.tust.2021.104301

Xie, Y., Liu, X., Zhang, C., Zhao, J., & Wang, H. (2021). Coupled heat transfer model for the combustion and steam characteristics of coal-fired boilers. *Engineering Applications of Computational Fluid Mechanics*, *15*, 490–502. https://doi.org/10.1080/19942060.2021.1890227

Xiong, C., Fan, H., Huang, X., & Fernandez-Pello, C. (2022). Evaluation of burning rate in microgravity based on the fuel regression, flame area, and spread rate. *Combustion and Flame*, *237*, 111846. https://doi.org/10.1016/j.combustflame.2021.111846

Yellapantula, S., Perry, B. A., & Grout, R. W. (2021). Deep learning-based model for progress variable dissipation rate in turbulent premixed flames. *Proceedings of the Combustion Institute*, *38*(2), 2929–2938. https://doi.org/10.1016/j.proci.2020.06.205

Zhang, T., Wang, Z., Wong, H. Y., Tam, W. C., Huang, X., & Xiao, F. (2022). Real-time forecast of compartment fire and flashover based on deep learning. *Fire Safety Journal*, *130*, 103579. https://doi.org/10.1016/j.firesaf.2022.103579

Zhang, T., Wang, Z., Zeng, Y., Wu, X., Huang, X., & Xiao, F. (2022). Building Artificial-Intelligence Digital Fire (AID-Fire) system: A real-scale demonstration. *Journal of Building Engineering*, *62*, 105363. https://doi.org/10.1016/j.jobe.2022.105363

Zhang, Y., Zhang, W., Lin, Y., Chen, Y., & Li, K. (2021). Flame attachment effect on the distributions of flow, temperature and heat flux of inclined fire plume. *International Journal of Heat and Mass Transfer*, *174*, 121313. https://doi.org/10.1016/j.ijheatmasstransfer.2021.121313